NASA TECHNICAL NOTE

C. 1

NASA TN D-5540

COLLECTIVE MOTIONS OF A ONE-DIMENSIONAL SELF-GRAVITATING SYSTEM

by Frank Hohl and Janet W. Campbell

Langley Research Center
Langley Station, Hampton, Va.

NATIONAL AERONAUTICS AND SPACE ADMINISTRATION • WASHINGTON, D. C. • NOVEMBER 1969

1. Report No. NASA TN D-5540	2. Government Accession No.	3. Recipient's Catalog No.
4. Title and Subtitle COLLECTIVE MOTIONS OF A ONE-DIMENSIONAL SELF-GRAVITATING SYSTEM		5. Report Date November 1969
		6. Performing Organization Code
7. Author(s) Frank Hohl and Janet W. Campbell		8. Performing Organization Report No. L-6846
9. Performing Organization Name and Address NASA Langley Research Center Hampton, Va. 23365		10. Work Unit No. 129-02-22-01-23
		11. Contract or Grant No.
12. Sponsoring Agency Name and Address National Aeronautics and Space Administration Washington, D.C. 20546		13. Type of Report and Period Covered Technical Note
		14. Sponsoring Agency Code

15. Supplementary Notes

16. Abstract

A one-dimensional computer model for a collisionless, self-gravitating system is used to investigate the mixing phase during which a stellar system approaches a quasi-equilibrium state. The results of the calculations are compared with the theory of the mixing phase proposed by Lynden-Bell. Previous investigations have shown that for simple initial conditions, the quasi-equilibrium state which is reached after several crossing times is close to the distribution predicted by Lynden-Bell. In the present paper, more complicated initial conditions are used to test the Lynden-Bell theory. For most systems investigated, the final state is close to the Lynden-Bell distribution. One exception is noted.

17. Key Words Suggested by Author(s) Statistical mechanics Collisionless relaxation Self-gravitating systems		18. Distribution Statement Unclassified – Unlimited		
19. Security Classif. (of this report) Unclassified	20. Security Classif. (of this page) Unclassified		21. No. of Pages 27	22. Price* $3.00

COLLECTIVE MOTIONS OF A ONE-DIMENSIONAL
SELF-GRAVITATING SYSTEM

By Frank Hohl and Janet W. Campbell
Langley Research Center

SUMMARY

A one-dimensional computer model for a collisionless, self-gravitating system is used to investigate the mixing phase during which a stellar system approaches a quasi-equilibrium state. The results of the calculations are compared with the theory of the mixing phase proposed by Lynden-Bell. Previous investigations have shown that for simple (uniform phase density) initial conditions the quasi-equilibrium state, which is reached after several crossing times, is close to the distribution predicted by Lynden-Bell. In the present paper more complicated initial conditions (two-phase density systems) are used to test the Lynden-Bell theory. For most systems investigated, the final state is close to the Lynden-Bell distribution. One exception is noted.

INTRODUCTION

In considering the evolution of stellar systems, the two fundamental time scales of interest are the crossing time τ_c and the thermalization time τ_r. The crossing time is associated with the collective motions of the stellar system and the thermalization time is associated with the binary interactions (collisions) of the individual stars. The crossing period is

$$\tau_c = \frac{2\pi}{\sqrt{4\pi G\rho}}$$

where G is the gravitational constant and ρ is the mass density. The mixing phase during which a collisionless system tends to approach a quasi-equilibrium state is of the order of τ_c. For the systems considered in the present report, the thermalization time is much larger than the crossing time, $\tau_r \gg \tau_c$. Thus, the mixing phase is well separated from the thermalization phenomena.

Recently, Lynden-Bell (ref. 1) proposed a theory of the mixing phase during which a collisionless stellar system approaches a quasi-equilibrium state. By using a new type of statistics related to Fermi-Dirac statistics, he derived a final or quasi-equilibrium distribution. In the present paper, computer experiments with a one-dimensional sheet

model (refs. 2 to 4) are performed to determine how closely a collisionless self-gravitating system will approach the Lynden-Bell distribution. The case for the most simple initial conditions (uniform phase density) has previously been investigated (ref. 5). These results showed that from 80 percent to 96 percent of the stars in the system approached the Lynden-Bell distribution. Similar results for the uniform initial phase density case were obtained by Cohen and Lecar (ref. 6). Hénon (ref. 7) used a model of concentric spherical mass shells to test the Lynden-Bell theory for the simple uniform-phase-density case and also obtained essentially the same results. It was found previously (ref. 8) that for the case of a plasma, an initially uniform phase-density system will approach the Lynden-Bell distribution.

For the simple case of an initially uniform phase-density distribution, the final state of the system is close to the distribution predicted by Lynden-Bell. It is of interest to determine whether more complicated initial distributions also approach the Lynden-Bell distribution.

The present investigation includes initial conditions having two different phase densities. Also, effects of the presence of different mass groups are investigated.

SYMBOLS

E	gravitational field
$f(x,v)$	distribution function, phase space density
$F(\epsilon)$	energy distribution function
G	gravitational constant
m	mass or mass per unit area
N	total number of stars in system
P	potential energy
T	kinetic energy
t	time
v	velocity

x	position coordinate
β	$1/\beta$ corresponds to a "temperature"
ϵ	total energy per unit mass
η	initial phase density
μ	"Fermi energy"
τ_c	crossing time
τ_{c0}	crossing time at $t = 0$
τ_r	thermalization time
φ	gravitational potential
$\langle\ \rangle$	averaged quantity

Subscripts:

i,j	summation indices
1,2	describes two different phase-density regions

STATISTICS

The equations describing a one-dimensional collisionless system are the collisionless Boltzmann equation

$$\frac{\partial f}{\partial t} + v\frac{\partial f}{\partial x} - \frac{\partial \varphi}{\partial x}\frac{\partial f}{\partial v} = 0 \tag{1}$$

and the Poisson equation

$$\nabla^2 \varphi = 4\pi G \int f\, dv \tag{2}$$

The most probable final state for a system described by equations (1) and (2) was recently discussed by Lynden-Bell (ref. 1). He assumes the phase space to be divided into a large

number of elements of phase f_i. He then argues that because of the large number of equivalent elements and the violent changes in the mean field, any distinct distribution of elements of phase is equally likely to occur subject to the conditions that the total energy and the number of elements of phase with a given initial density are conserved. The elements of phase f_i are distinguishable. According to equation (1), the elements of phase cannot overlap and, therefore, follow an exclusion principle. Such a phase fluid should obey a fourth type of statistics which, in general, is different from that of Maxwell-Boltzmann, Bose-Einstein, and Fermi-Dirac. By evaluating the most probable distribution of elements of phase, Lynden-Bell obtains the coarse-grained (macroscopic) distribution

$$\langle f \rangle = \sum_j \eta_j \frac{\exp\left[-\beta_j(\epsilon - \mu_j)\right]}{1 + \sum_j \exp\left[-\beta_j(\epsilon - \mu_j)\right]} \tag{3}$$

where the summation occurs because initially there are elements of phase with different densities η_j.

For the special case where the initial f has a constant value η over certain regions of phase space and is zero outside these regions (water-bag distribution), the distribution reduces to

$$\langle f \rangle = \frac{\eta}{1 + \exp\left[\beta(\epsilon - \mu)\right]} \tag{4}$$

where ϵ is the total energy of a star and the two constants β and μ are determined by the conservation of energy and area in phase space. The distribution given by equation (4) is formally identical with the Fermi-Dirac distribution. The parameter μ corresponds to the Fermi energy, whereas the parameter $1/\beta$ corresponds to a "temperature" and is a measure of the excitation above the minimum energy state corresponding to $1/\beta = 0$. This minimum-energy state is discussed by Hohl and Feix (refs. 4 and 9) for the case of a one-dimensional system and in this paper is referred to as the stationary state.

Equation (4) can be written in the form

$$\beta(\epsilon - \mu) = \log_e\left(\frac{\langle f \rangle}{\eta - \langle f \rangle}\right) \tag{5}$$

so that a plot of $\log_e\left[\langle f \rangle / \left(\eta - \langle f \rangle\right)\right]$ as a function of energy should give a straight line. For a highly nondegenerate system such as that investigated by Buneman (ref. 2) $\langle f \rangle \ll \eta$, and the distribution given by equation (4) will approach a Maxwellian. On the other hand,

4

a distribution near the stationary state of a single contour water-bag distribution (refs. 4 to 6) corresponds to a low-temperature ($1/\beta \approx 0$) Fermi distribution. For the case of a system with two different initial-phase densities η_1 and η_2, the following relationships hold (appendix I of ref. 1)

$$\langle f_1 \rangle = \eta_1 \frac{\exp\left[-\beta_1(\epsilon - \mu_1)\right]}{1 + \exp\left[-\beta_1(\epsilon - \mu_1)\right] + \exp\left[-\beta_2(\epsilon - \mu_2)\right]} \tag{6}$$

and

$$\langle f_2 \rangle = \eta_2 \frac{\exp\left[-\beta_2(\epsilon - \mu_2)\right]}{1 + \exp\left[-\beta_1(\epsilon - \mu_1)\right] + \exp\left[-\beta_2(\epsilon - \mu_2)\right]} \tag{7}$$

or

$$\beta_1(\epsilon - \mu_1) = \log_e\left[\frac{\langle f_1 \rangle}{\eta_1\left(1 - \frac{\langle f_1 \rangle}{\eta_1} - \frac{\langle f_2 \rangle}{\eta_2}\right)}\right] \tag{8}$$

and

$$\beta_2(\epsilon - \mu_2) = \log_e\left[\frac{\langle f_2 \rangle}{\eta_2\left(1 - \frac{\langle f_1 \rangle}{\eta_1} - \frac{\langle f_2 \rangle}{\eta_2}\right)}\right] \tag{9}$$

THE MODEL

A one-dimensional sheet model (refs. 2 to 4) was used for the computer simulation of the mixing phase of collisionless systems. Consider a system of N mass sheets with ordered sheet positions $x_1, x_2, x_3, \ldots, x_n$ such that $x_j \leq x_{j+1}$. The gravitational field E_j acting on a sheet at x_j is obtained from the net mass to the left of x_j; that is,

$$E_j = 2\pi G \sum_{i=1}^{N} m_i \, \text{sgn}\left(x_j - x_i\right) \tag{10}$$

where m_i is the mass per unit area of the sheet at x_i and

$$\left.\begin{array}{ll} \text{sng}(x) = -1 & (x > 0) \\ \text{sgn}(x) = 0 & (x = 0) \\ \text{sgn}(x) = 1 & (x < 0) \end{array}\right\} \tag{11}$$

The velocity and position of the sheets are advanced stepwise in time by using the time-centered finite-difference equations

$$v\left(t + \frac{\delta t}{2}\right) = v\left(t - \frac{\delta t}{2}\right) + \delta t E(x,t) \tag{12}$$

and

$$x(t + \delta t) = x(t) + \delta t v\left(t + \frac{\delta t}{2}\right) \tag{13}$$

The process of ordering the sheets, calculating the field, and advancing velocities and position by a small time step δt is repeated until the desired evolution of the system is achieved.

RESULTS AND DISCUSSION

The Lynden-Bell theory of violent relaxation (ref. 1) does not account for any effects due to the presence of different mass groups. It is therefore important to ensure that no mass segregation occurs when different mass groups are present. The effect of the presence of two different mass groups was determined by repeating some of the calculations presented in reference 5, but by representing the upper stream (positive velocity stars) by 2000 mass sheets each of mass 1 (per unit area) and the lower stream by 1000 mass sheets each of mass 2. The resulting evolution of the system in phase space is shown in figure 1. The time is shown in crossing periods τ_{c0} calculated for the initial density. The initial distribution is equivalent to that of the system shown in figure 1 of reference 5. The evolution of the system shown in figure 5 of reference 5 was also repeated by replacing the upper stream by 2000 stars of mass 1/2 and the lower stream by 1000 stars of mass 1. Figure 2 shows the resulting evolution in phase space. The evolution displayed in figures 1 and 2 is practically identical to that shown in figures 1 and 5 of reference 5. Also, when $\log_e\left[\langle f \rangle / \left(\eta - \langle f \rangle\right)\right]$ is plotted separately for the light and heavy stars, a practically identical distribution is obtained for both cases. Each one of the plots of $\log_e\left[\langle f \rangle / \left(\eta - \langle f \rangle\right)\right]$ gives the same variations as the corresponding plot presented in reference 5 for the same initial phase-density system. Thus, the final distribution when two different mass groups are present is the same as that for the case when all sheets are of equal mass.

In figure 3 the percent kinetic-energy difference given by

$$\frac{\frac{1}{2}\sum_i m_i v_i^2 (\text{light stars}) - \frac{1}{2}\sum_i m_i v_i^2 (\text{heavy stars})}{\frac{1}{2}\sum_i m_i v_i^2 (\text{light stars}) + \frac{1}{2}\sum_i m_i v_i^2 (\text{heavy stars})} \times 100 \tag{14}$$

is plotted as a function of time for the two systems shown in figures 1 and 2. It can be seen that in spite of the large fluctuations, there is no apparent systematic increase in the kinetic energy of the light stars; that is, no equipartition of energy occurs on a time scale τ_c. These results are to be expected since Hohl and Broaddus (ref. 10) have found that the thermalization or relaxation effects for the one-dimensional model occur on a time scale

$$\tau_r \approx N^2 \tau_c \tag{15}$$

where N is the number of mass sheets in the system. Thus, during the process of violent relaxation as simulated by the one-dimensional model, purely collective inter- actions of the stars cause the system to approach its quasi-equilibrium state.

The evolution in phase space of the first two-phase-density systems investigated is shown in figure 4. Initially, the central region of the system bounded by $x = \pm 187.5$ and $v = \pm 375$ contains 1008 stars of mass 1. The two outer regions bounded by $x = \pm 187.5$, $x = \pm 375$, and $v = \pm 375$ each contain 1008 stars of mass 1. Therefore, the initial den- sity in the central region defined by f_1 is one-half that of the two outer regions defined by f_2.

To compare the final state of the system with the distribution given by equations (6) and (7), the phase space is divided into a number of cells. Each mass sheet represents a point in a cell in phase space. The average number of mass sheets per cell and the corresponding energy $\epsilon = \frac{1}{2}mv^2 + m\varphi$ are determined by averaging over several dis- tributions near the final time $t = 47.7\tau_{c0}$ as shown in figure 4. These calculations are done separately for stars corresponding to f_1 and to f_2. The cell size chosen was such that initially, the phase densities (mass per cell) corresponding to f_1 and f_2 were $\eta_1 = 20.16$ and $\eta_2 = 40.32$.

Figure 5 shows the variation of the distributions $\langle f_1 \rangle$, $\langle f_2 \rangle$, and $\langle f \rangle = \langle f_1 + f_2 \rangle$ as a function of energy. Also shown as inserts in the same figure are F_1, F_2, and F which are the distributions of the mass per energy interval corresponding to $\langle f_1 \rangle$, $\langle f_2 \rangle$, and $\langle f \rangle$, respectively. The normalizations

$$\int f \, dx \, dv = 1$$

$$\int f_1 \, dx \, dv = 1$$

$$\int f_2 \, dx \, dv = 1$$

and

$$\int F \, d\epsilon = 3 \times 10^4$$

$$\int F_1 \, d\epsilon = 3 \times 10^4$$

$$\int F_2 \, d\epsilon = 3 \times 10^4$$

are used throughout the present paper. The dots shown in figure 5 are the numerical results obtained from the computer calculations. The solid curves represent the Lynden-Bell distribution which gives the best fit to the numerical data; that is, the quantity $\sum_i \left[f_i(\text{theory}) - f_i(\text{numerical}) \right]^2$ is minimized. For high energies the value of $\langle f \rangle$ is too large and in obtaining the fit the high-energy bump in the distribution was neglected. This high-energy bump in the distribution was also obtained by Hénon in his spherical shell model (ref. 7). Lynden-Bell (ref. 11) suggests that this deviation occurs because the high-energy stars have a large period and remain outside the main system for a longer time than the low-energy stars. When the high-energy stars return to the center of the system, the system has nearly reached a steady state and the mechanism for phase mixing would no longer be effective. The values of the constants β_1, β_2, μ_1, and μ_2 corresponding to the "best" fit shown in figure 5 are also given in figure 5. One of the difficulties of the Lynden-Bell distribution is that the parameters of the final state cannot be calculated in advance. Nevertheless, the results presented in figure 5 show that the final state can be closely approximated by the Lynden-Bell distribution. The dip in $\langle f_2 \rangle$ obtained from the numerical results can be explained in terms of the initial distribution. Initially, the central part has a low phase density and as the system evolves, the outer higher phase density tries to displace the lower central density. Since the two-phase densities cannot pass through each other (exclusion principle), some portions of the lighter region are trapped near the center of the system, and thereby stars corresponding to the heavier phase density are prevented from occupying this region. The result is a lower phase density in the central region as shown in figure 5. In the previous investigation (ref. 5) of single-phase density systems, equation (5) was used for comparing the computer results with the Lynden-Bell distribution. An attempt was made to use equations (8) and (9) for the present two-phase density cases. However, the numerically obtained deviations from the Lynden-Bell distribution for small energies (as shown in fig. 5) caused large variations in the logarithmic terms and the results were misleading. For this reason equations (6) and (7) are used.

The evolution of the kinetic energy for the system shown in figure 4 is given in figure 6. Initially, the total potential energy P is nearly 10 times the total kinetic energy T. However, after a short time, the virial theorem is satisfied (if the average is taken over the oscillation in the energies) and $2T = P$.

The evolution in phase space for the next case is shown in figure 7. Initially, the region bounded by $x = 0$, $x = -250$, and $v = \pm312.5$ contains 1000 stars of mass 1.6, and the region bounded by $x = 0$, $x = 250$, and $v = \pm312.5$ contains 1000 stars of mass 0.4. Thus, the left-hand region corresponding to f_2 has an initial phase density four times as large as the right-hand region which corresponds to f_1. Also, the heavy stars are represented by small rectangles and the light stars by small circles. It can be seen that most of the high-energy stars are light stars. The corresponding distribution functions obtained near $t = 47.7\tau_{c0}$ are shown in figure 8. For this case the "best" fit was obtained by including all the high-energy bumps. The total distribution $\langle f \rangle$ and also $\langle f_2 \rangle$ are fairly well represented by the Lynden-Bell distribution. However, the two peaks in $\langle f_1 \rangle$ are probably caused again by a combination of trapping between regions of $\langle f_1 \rangle$ and by nonmixing of high-energy stars. The evolution of the kinetic energy for the same system is shown in figure 9. Initially, the potential energy is four times the kinetic energy but the energies quickly reach the point where they oscillate around $P = 2T$.

The next case investigated is one where a region of heavy phase density completely encloses a region of low phase density. The evolution in phase space for this system is shown in figure 10. The central rectangle defined by $x = \pm177$ and $v = \pm177$ contains 1000 stars each of mass 0.5. The outer region exterior to the central rectangle and enclosed by $x = \pm250$ and $v = \pm250$ contains 1000 stars each of mass 1.5. The two regions have equal areas so that the outer region corresponding to f_2 has a phase density which is three times as large as the phase density in the central region which corresponds to f_1. Figure 10 shows that nearly all the high-energy stars are heavy stars represented by small rectangles (corresponding to f_2). This result was to be expected since stars from the inner regions (corresponding to f_1) cannot penetrate the outer region f_2. Thus, again the light region is trapped near the center of the system. Another point to note is illustrated by the stage of the evolution at $t = 3.2\tau_{c0}$ in figure 10. It can be seen that parts of the outer region have condensed into two clusters which displace some of the lighter regions away from the central part of the system. However, these displaced regions are still trapped inside regions of f_2. Figure 11 shows a comparison of the distribution functions of this system with the Lynden-Bell distribution after the system has reached the quasi-equilibrium state. The results are essentially the same as those for the previous two cases; that is, most of the stars follow the Lynden-Bell distribution. The variation of the kinetic energy for the system is shown

in figure 12. Initially, the potential energy of the system is almost four times as large as the total kinetic energy.

The final system investigated is shown in figure 13. The top and the bottom rectangle are defined by $x = \pm 83.3$, $v = \pm 83.3$, and $v = \pm 250$ and each of the two rectangles contains 506 stars of mass 0.4 represented by a circle. The right and left rectangles are defined by $x = \pm 83.3$, $x = \pm 250$, and $v = \pm 83.3$ and each of the two rectangles contains 506 stars of mass 1.6 represented by a small rectangle. The region of phase space covered by the right and left rectangle corresponds to f_2 and has a phase density four times as large as the top and bottom rectangles which correspond to f_1. Compared with the previous three cases, the system has a rather large initial ratio of potential to kinetic energy; the initial potential energy is 23 times as large as the total initial kinetic energy. Figure 14 shows the final distribution functions for the system obtained near $t = 47.7\tau_{c0}$. The variation of the kinetic energy for this system is shown in figure 15. For this system it is not possible to obtain any reasonable fit of the numerical results with the Lynden-Bell distribution. The relaxation is certainly very violent as required by the Lynden-Bell theory.

However, from the dynamics of the system as displayed in figure 13 it can be seen that the final state of the system is rather purely mixed. Initially the two heavy-phase density rectangles tend to fall toward the center of the system and most of the stars corresponding to the low-phase-density regions are displayed toward higher energies. In fact, up to a time $t = 4.0\tau_{c0}$, the system rotates (in phase space) like a binary system with the heavy-phase-density regions continually approaching each other. At the same time, the low-phase-density regions are being pushed to higher energies. At $t = 8.0\tau_{c0}$, the two heavy regions have merged and occupy the central region of the system. Only very few of the stars corresponding to the initial-low-phase-density regions are near the center of the system. This state of the system corresponds, of course, to the distributions shown in figure 14. These results indicate that if the final state is to be described by the Lynden-Bell distribution, the evolution of the system must proceed with sufficient interpenetration of regions of different phase density.

For the single-phase-density case, the stationary state is always stable and is described by a zero-temperature $(1/\beta \approx 0)$ Fermi-Dirac distribution. In studying the evolution of such single-phase-density systems, it was found (refs. 4 and 9) that within the limitations of energy conservation, the system approaches the stationary state. Since the Lynden-Bell distribution reduces to the Fermi-Dirac distribution for this simple case, one would expect the final state of the system to be approximated by the Lynden-Bell distribution. Consider now the case of a multiphase density system (refs. 9 and 12). A stable stationary two-phase-density system is described by

$$f_1(\epsilon) = \eta_1 \qquad\qquad\qquad (0 \leqq \epsilon \leqq \mu)$$

$$f_1(\epsilon) = 0 \qquad\qquad\qquad (\epsilon > \mu)$$

and

$$f_2(\epsilon) = \eta_2 \qquad\qquad\qquad \left(\mu_1 < \epsilon \leqq \mu_2\right)$$

$$f_2(\epsilon) = 0 \qquad\qquad\qquad \left(\epsilon < \mu_1; \; \epsilon > \mu_2\right)$$

where $\eta_1 > \eta_2$. In terms of Fermi-Dirac distribution, f_1 and f_2 can be written as

$$f_1(\epsilon) = \eta_1 \frac{\exp\left[-\beta_1(\epsilon - \mu_1)\right]}{1 + \exp\left[-\beta_1(\epsilon - \mu_1)\right]} \tag{16}$$

and

$$f_2(\epsilon) = \eta_2 \left\{ \frac{\exp\left[-\beta_2(\epsilon - \mu_2)\right]}{1 + \exp\left[-\beta_2(\epsilon - \mu_2)\right]} - \frac{\exp\left[-\beta_1(\epsilon - \mu_1)\right]}{1 + \exp\left[-\beta_1(\epsilon - \mu_1)\right]} \right\} \tag{17}$$

where $1/\beta_1 \approx 0$ and $1/\beta_2 \approx 0$. Equations (16) and (17) give a better approximation of the final state of the system shown in figures 13 and 14 than the Lynden-Bell distribution.

CONCLUDING REMARKS

Since the motion of "stars" in the two-dimensional phase space is always bounded, the collisionless, one-dimensional model is well suited for a check of the Lynden-Bell theory. It was found that no mass segregation occurs when two different mass groups are present.

Most of the calculations with two different initial phase densities give results in good agreement with the Lynden-Bell distribution. The small deviations in these cases can be explained by considering the dynamics of the stars. For one case investigated, however, the final state of the two phase densities cannot even be approximated by the Lynden-Bell distribution. Since the Lynden-Bell distribution is obtained without actually considering the dynamics of the stars, it is surprising that for most of the systems investigated, the final state does correspond to a Lynden-Bell distribution. One of the

disadvantages of the Lynden-Bell distribution is that the parameters of the final state cannot be calculated in advance.

Langley Research Center,
National Aeronautics and Space Administration,
Langley Station, Hampton, Va., September 19, 1969.

REFERENCES

1. Lynden-Bell, D.: Statistical Mechanics of Violent Relaxation in Stellar Systems. Mon. Notic. Roy. Astron. Soc., vol. 136, no. 1, 1967, pp. 101-121.

2. Buneman, O.: Dissipation of Currents in Ionized Media. Phys. Rev., Second ser., vol. 115, no. 3, Aug. 1, 1959, pp. 503-517.

3. Dawson, John: One-Dimensional Plasma Model. Phys. Fluids, vol. 5, no. 4, Apr. 1962, pp. 445-459.

4. Hohl, Frank; and Feix, Marc R.: Numerical Experiments With a One-Dimensional Model for a Self-Gravitating Star System. Astrophys. J., vol. 147, no. 3, Mar. 1967, pp. 1164-1180.

5. Hohl, Frank; and Campbell, Janet W.: Statistical Mechanics of a Collisionless Self-Gravitating System. Astron. J., vol. 73, no. 7, Sept. 1968, pp. 611-615.

6. Cohen, Léon; and Lecar, Myron: Approach to Equilibrium of a One Dimensional Self Gravitating System. Bull. Astron., 3e ser., tome III, fasc. 2, 1968, pp. 213-225.

7. Hénon, Michel: Collective Motions in a Spherical Star Cluster. Bull. Astron., 3e ser., tome III, fasc. 2, 1968, pp. 241-264.

8. Hohl, Frank: Minimum Energy Property of a Bounded One-Dimensional Plasma. Phys. Fluids, vol. 12, no. 1, Jan. 1969, pp. 230-233.

9. Hohl, Frank: Theory and Results on Collective and Collisional Effects for a One-Dimensional Self-Gravitating System. NASA TR R-289, 1968.

10. Hohl, F.; and Broaddus, D. Tilghman: Thermalization Effects in a One-Dimensional Self-Gravitating System. Phys. Leters, vol. 25A, no. 10, Nov. 20, 1967, pp. 713-714.

11. Anon.: Résumé de la Communication de M. D. Lynden-Bell. Bull. Astron., 3e ser., tome II, fasc. 1, 1967, pp. 163-166.

12. Hohl, Frank; and Feix, M. R.: A Variational Principle for a One-Dimensional Stellar System. Astrophys. J., vol. 151, no. 2, pt. 1, Feb. 1968, pp. 783-788.

12
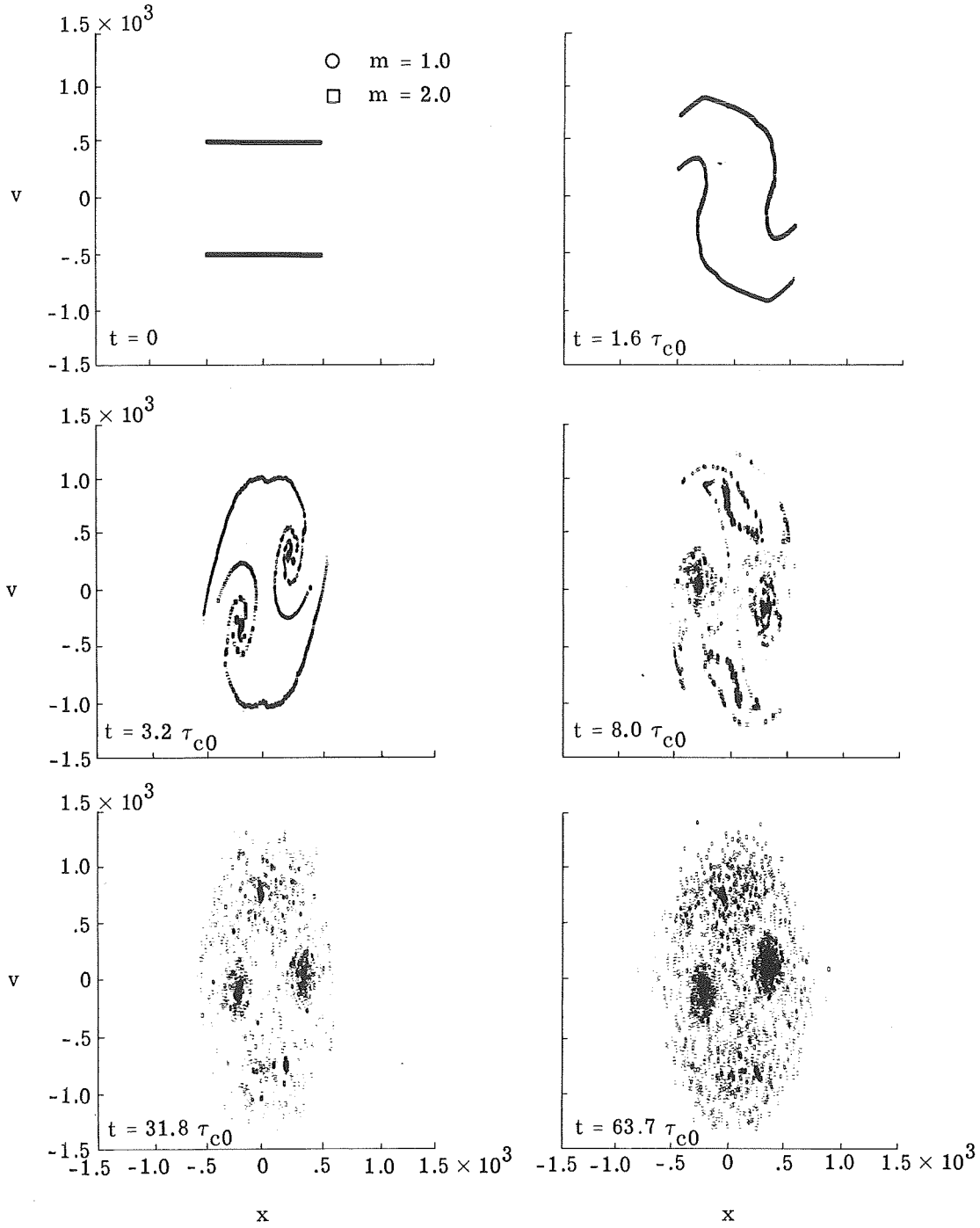
Figure 1.- Evolution in phase space of a system of two counterflowing streams of stars. The upper stream consists of 2000 stars of mass 1 each denoted by a small circle; the lower stream consists of 1000 stars of mass 2 each denoted by a small rectangle.
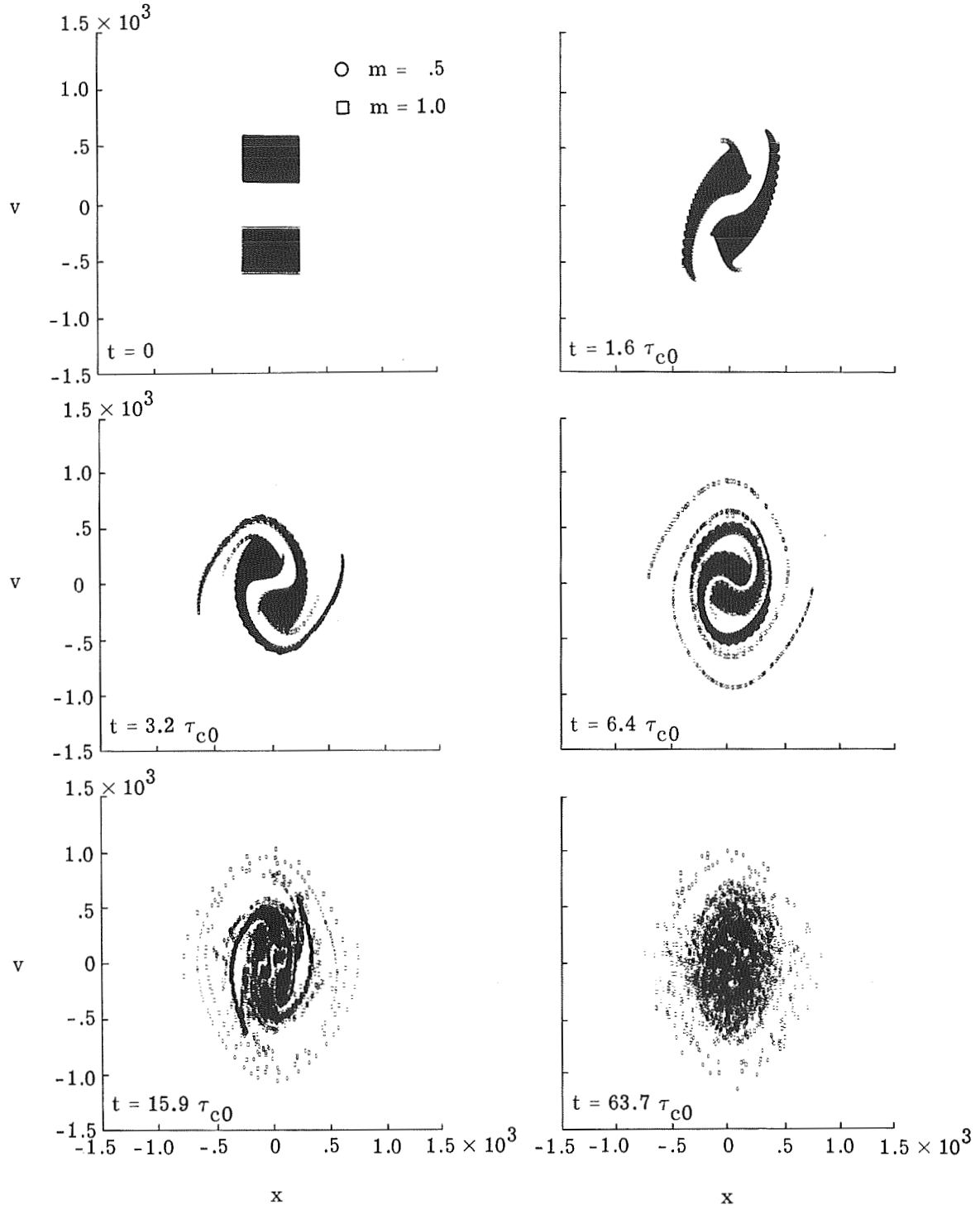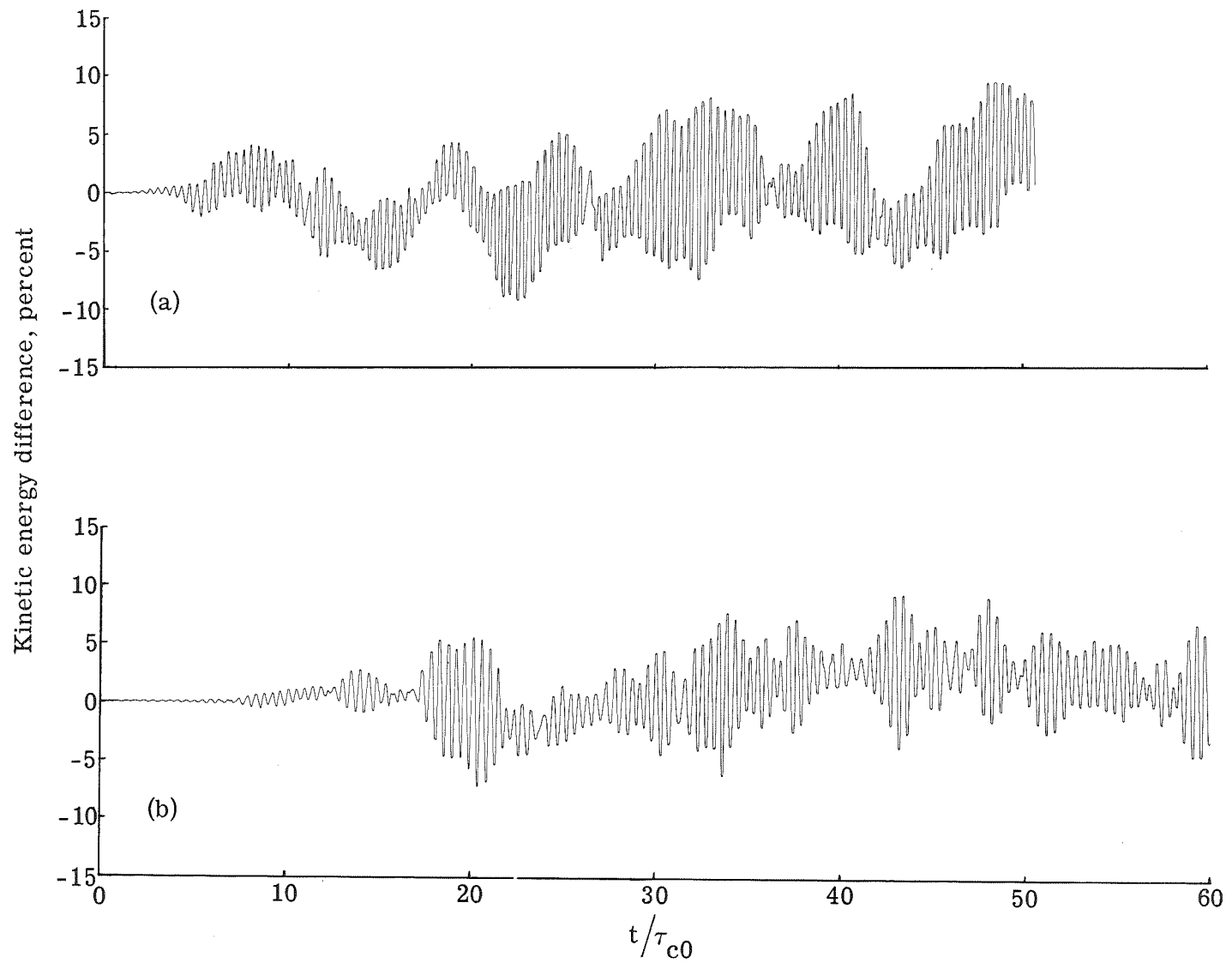
Figure 2.- Evolution in phase space of a system containing two mass groups. The upper rectangle consists of 2000 stars of mass 0.5, each denoted by a circle and the lower rectangle consists of 1000 stars of mass 1.0, each denoted by a rectangle.

14

Figure 3.- Evolution of the normalized kinetic energy difference between the heavy and the light stars: (a) For the system shown in figure 1 and (b) For the system shown in figure 2.
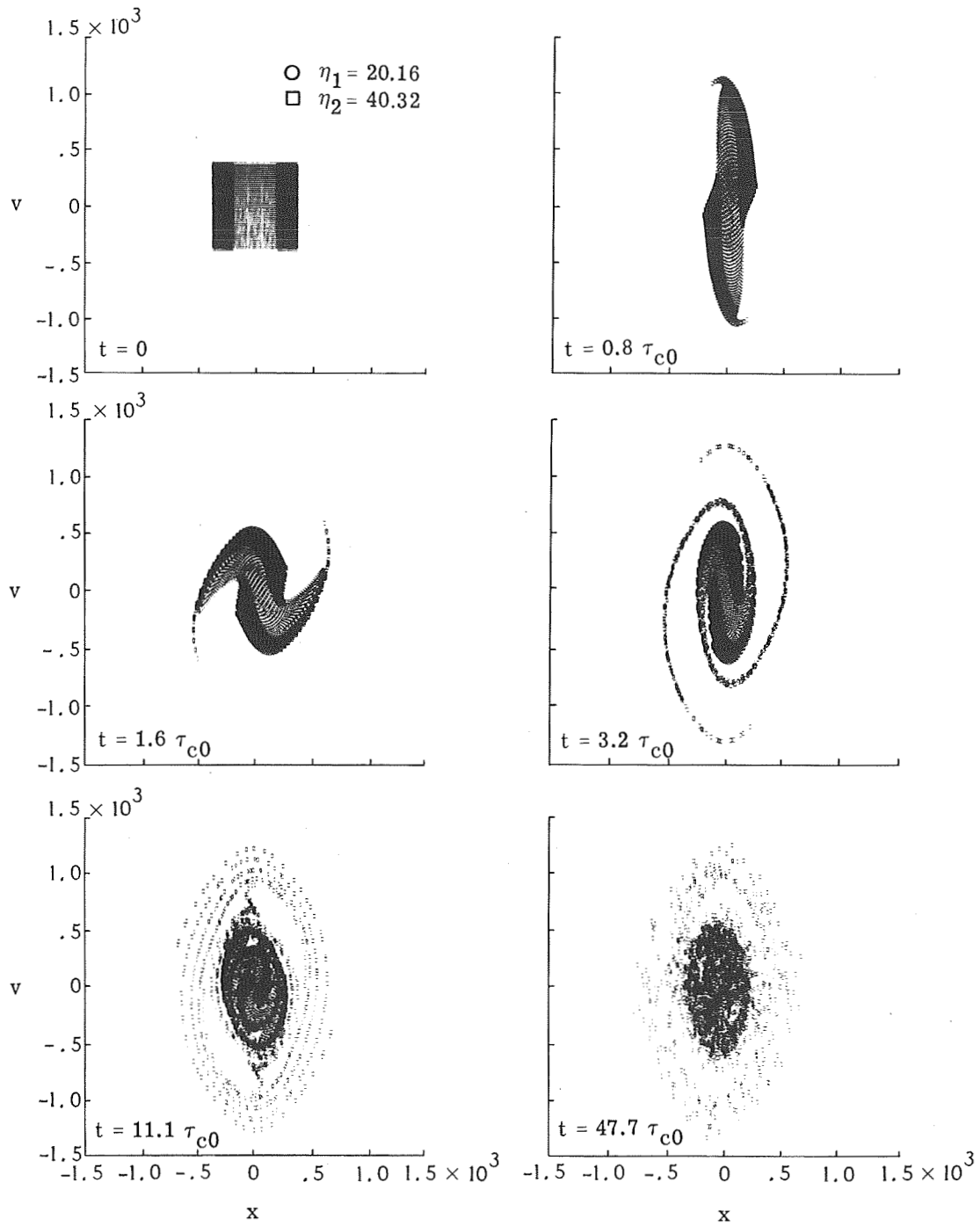
Figure 4.- Evolution of a two-phase-density system in phase space. The stars in the central part are denoted by small circles and those in the two outer regions by small rectangles. The central phase density corresponds to $\eta_1 = 20.16$ and the phase density in the outer regions corresponds to $\eta_2 = 40.32$.
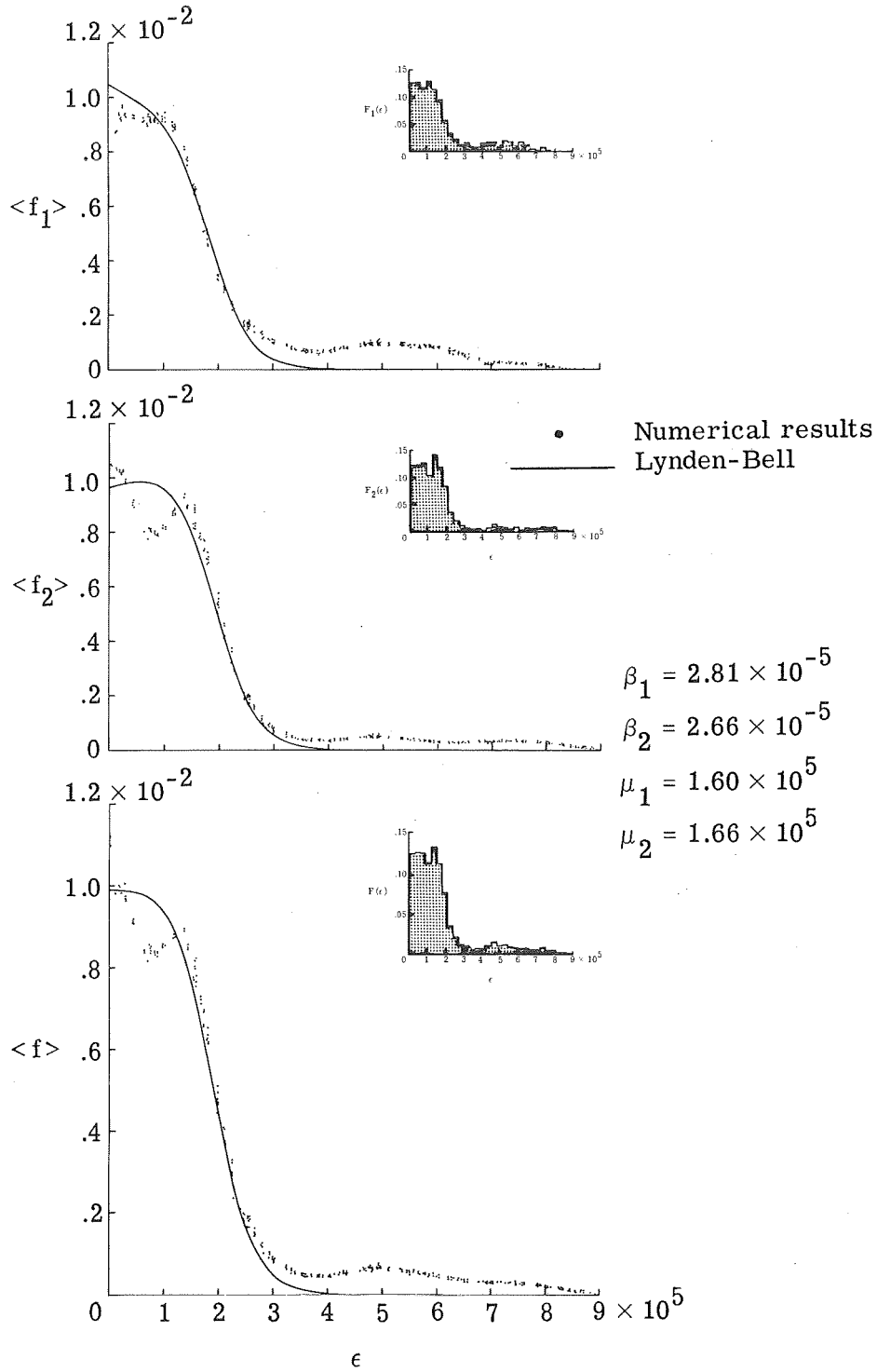
Figure 5.- Comparison of final distribution with the Lynden-Bell distribution for the system shown in figure 4. Inserts show the energy distribution.
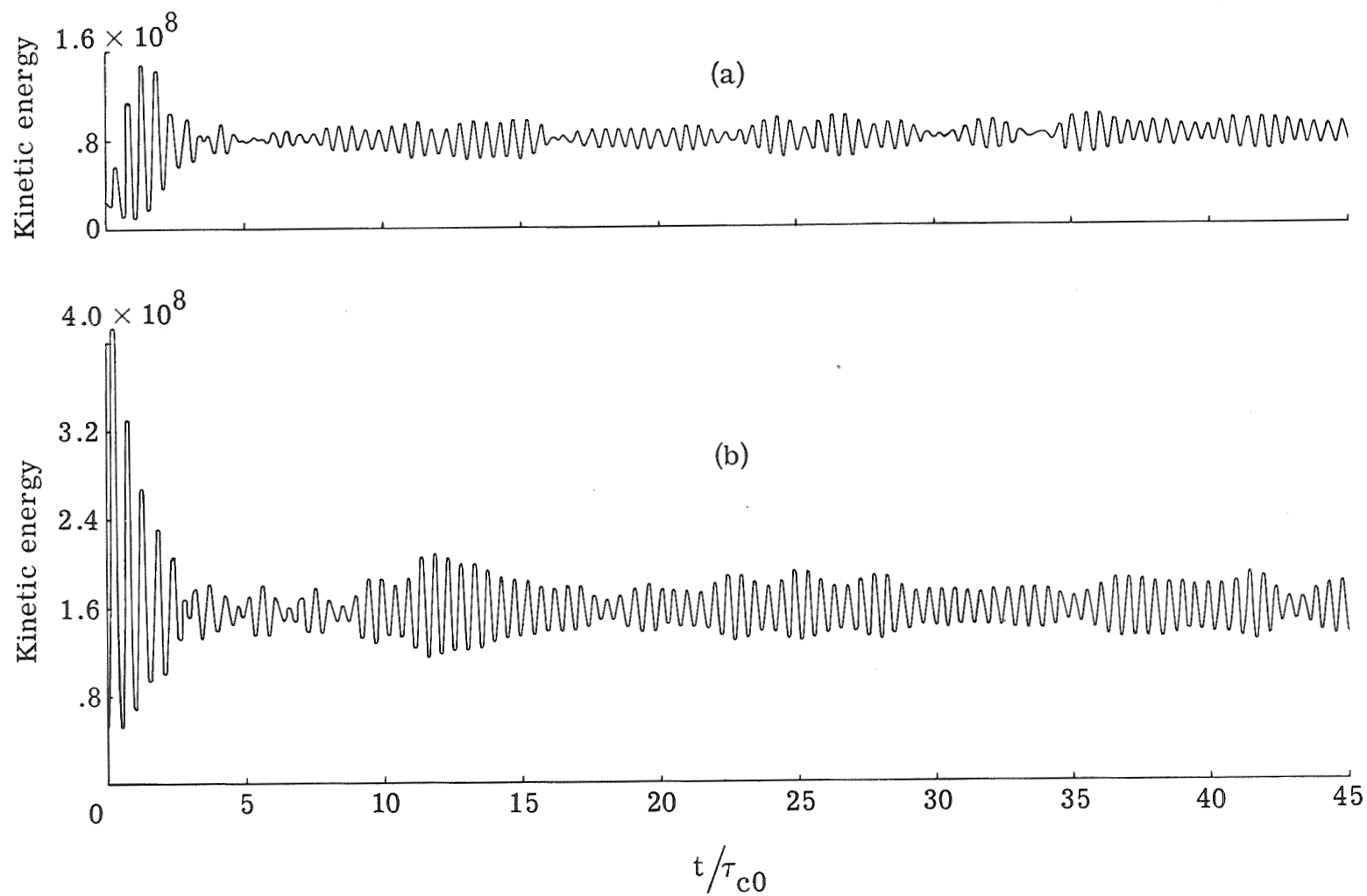
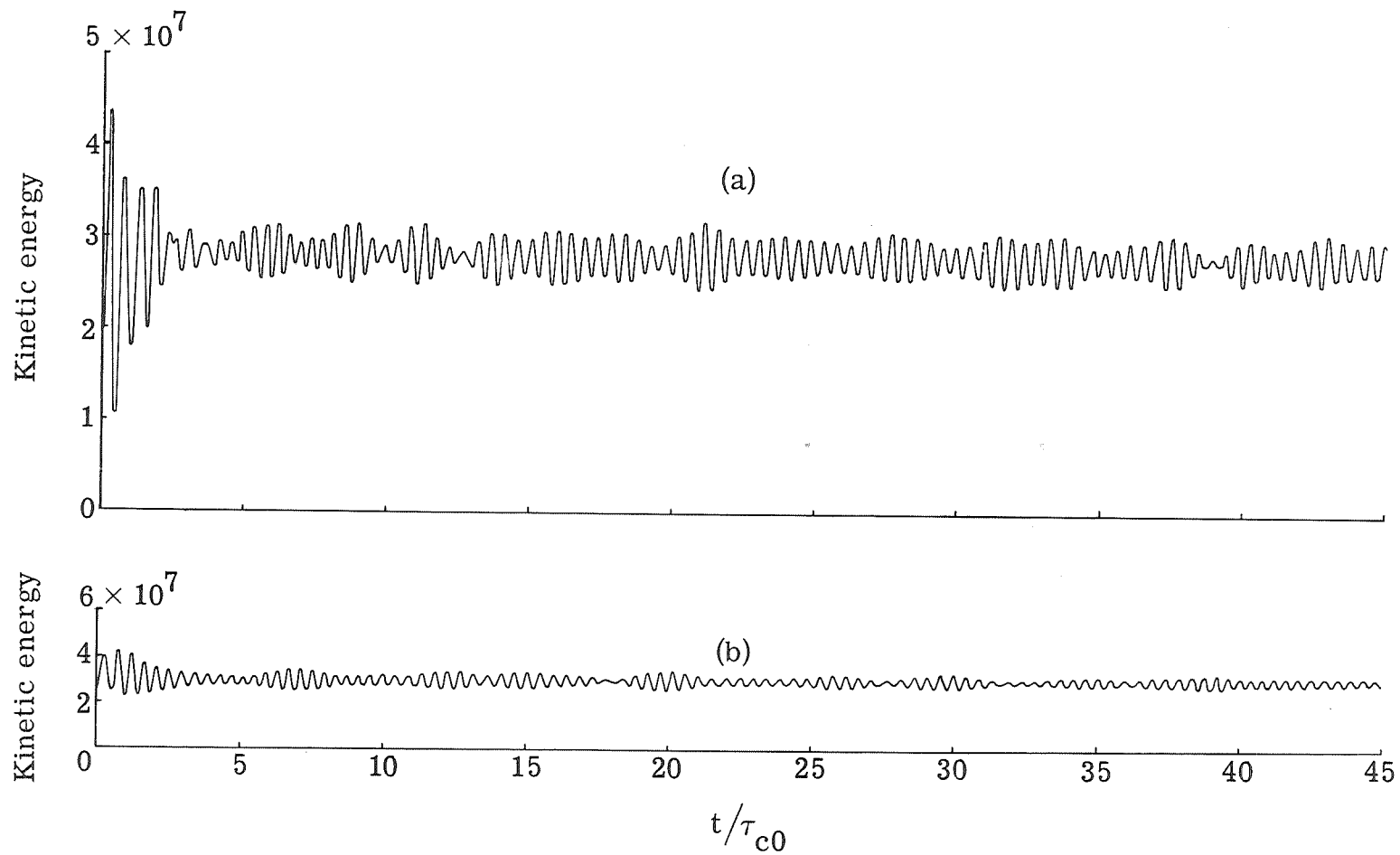Figure 6.- Evolution of the kinetic energy for the system shown in figure 4: (a) Total kinetic energy corresponding to stars in the light region f_1 and (b) Total kinetic energy corresponding to stars in the heavy region f_2.
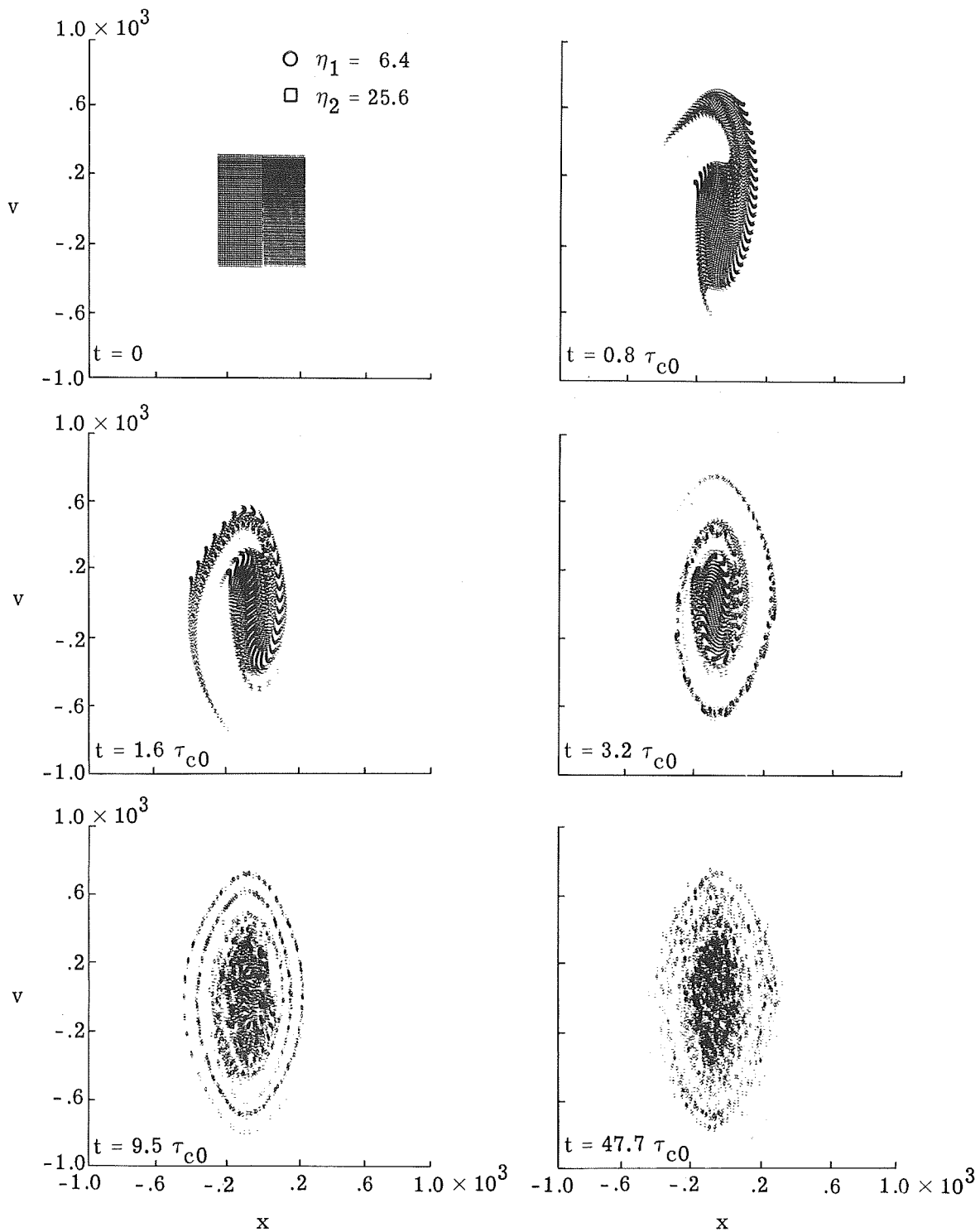
Figure 7.- Evolution of a two-phase-density system in phase space. The phase density in the left region is four times the phase density of the right region.
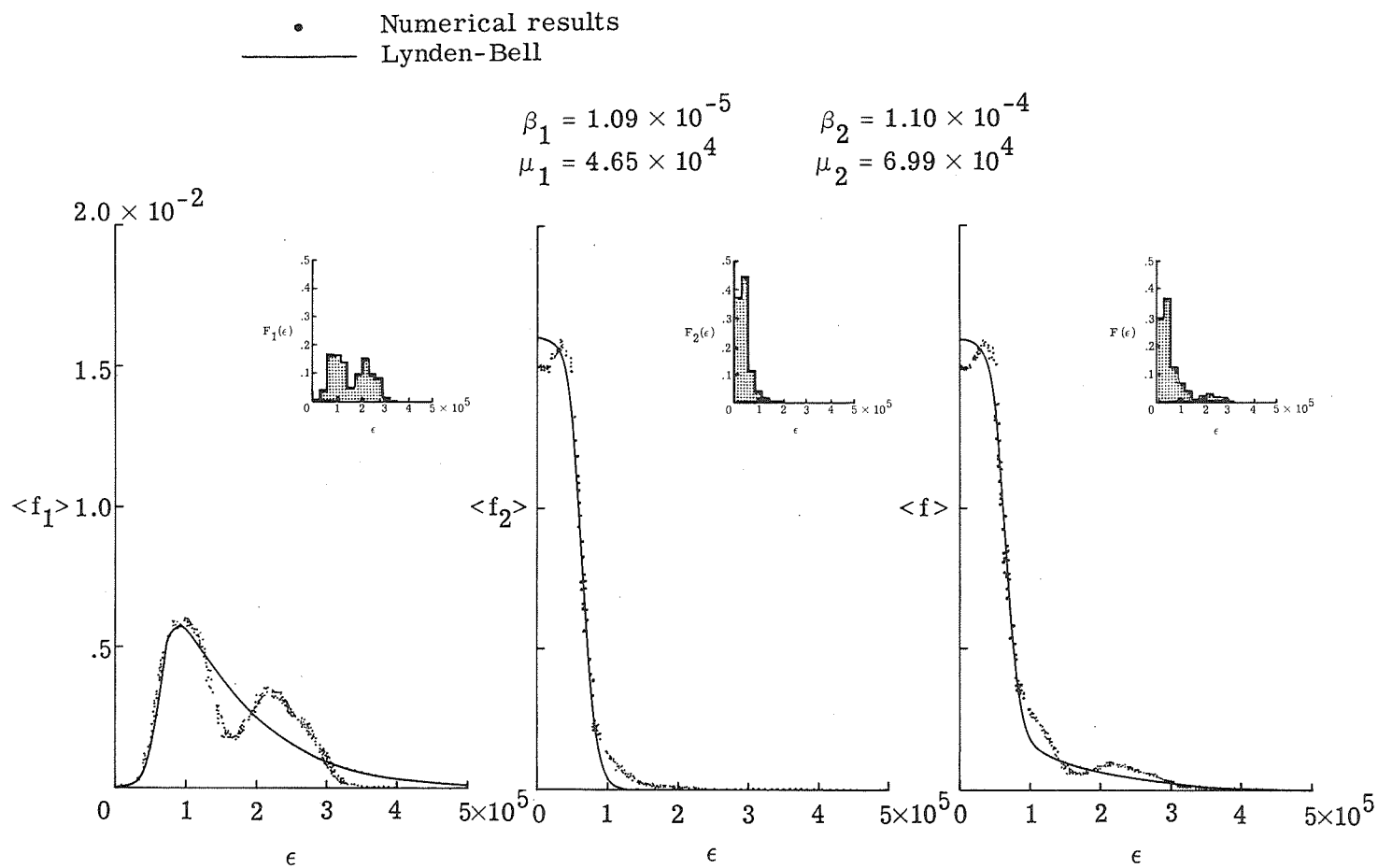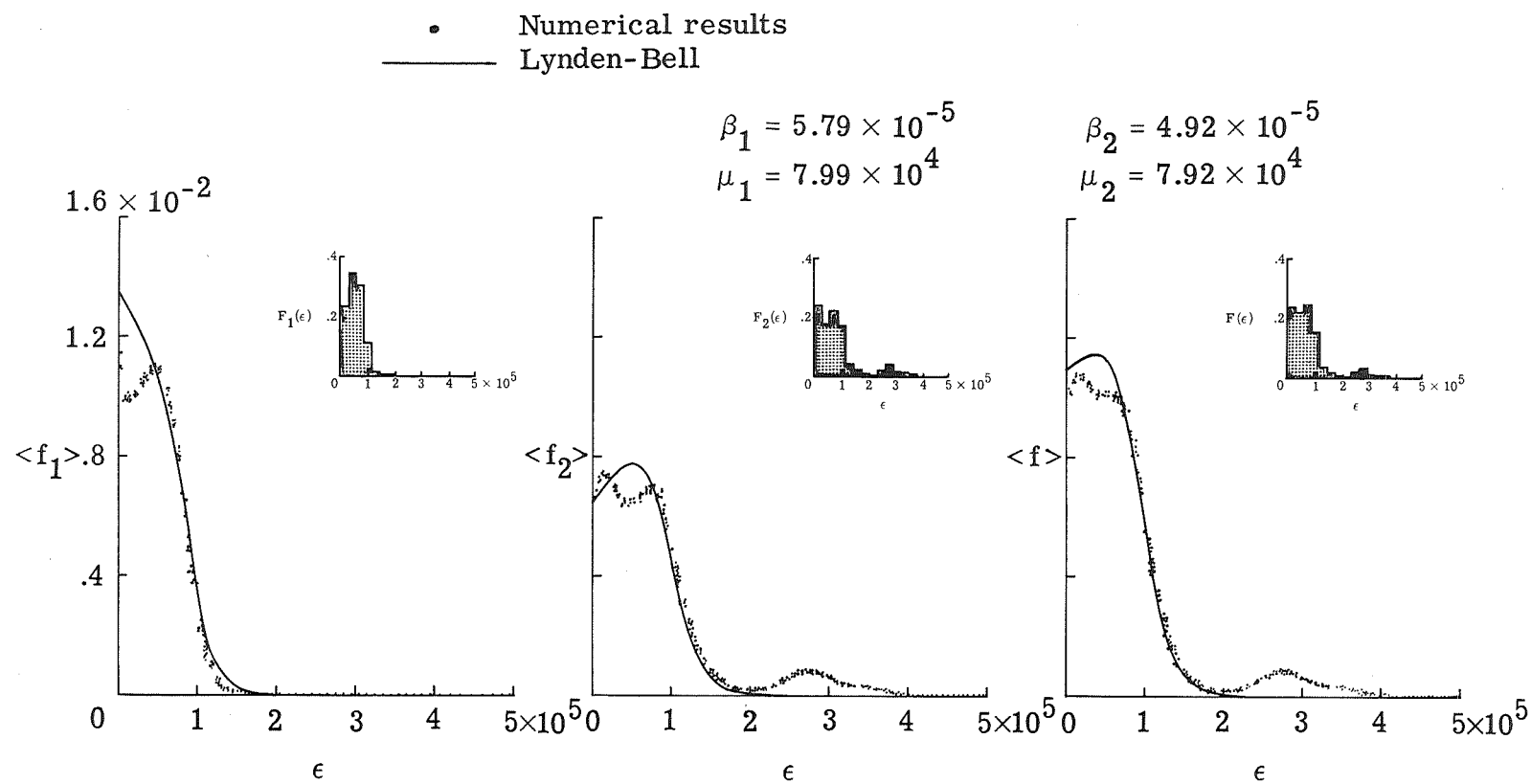
Figure 8.- Comparison of the final distribution with the Lynden-Bell distribution for the system shown in figure 7. Inserts show the energy distribution.
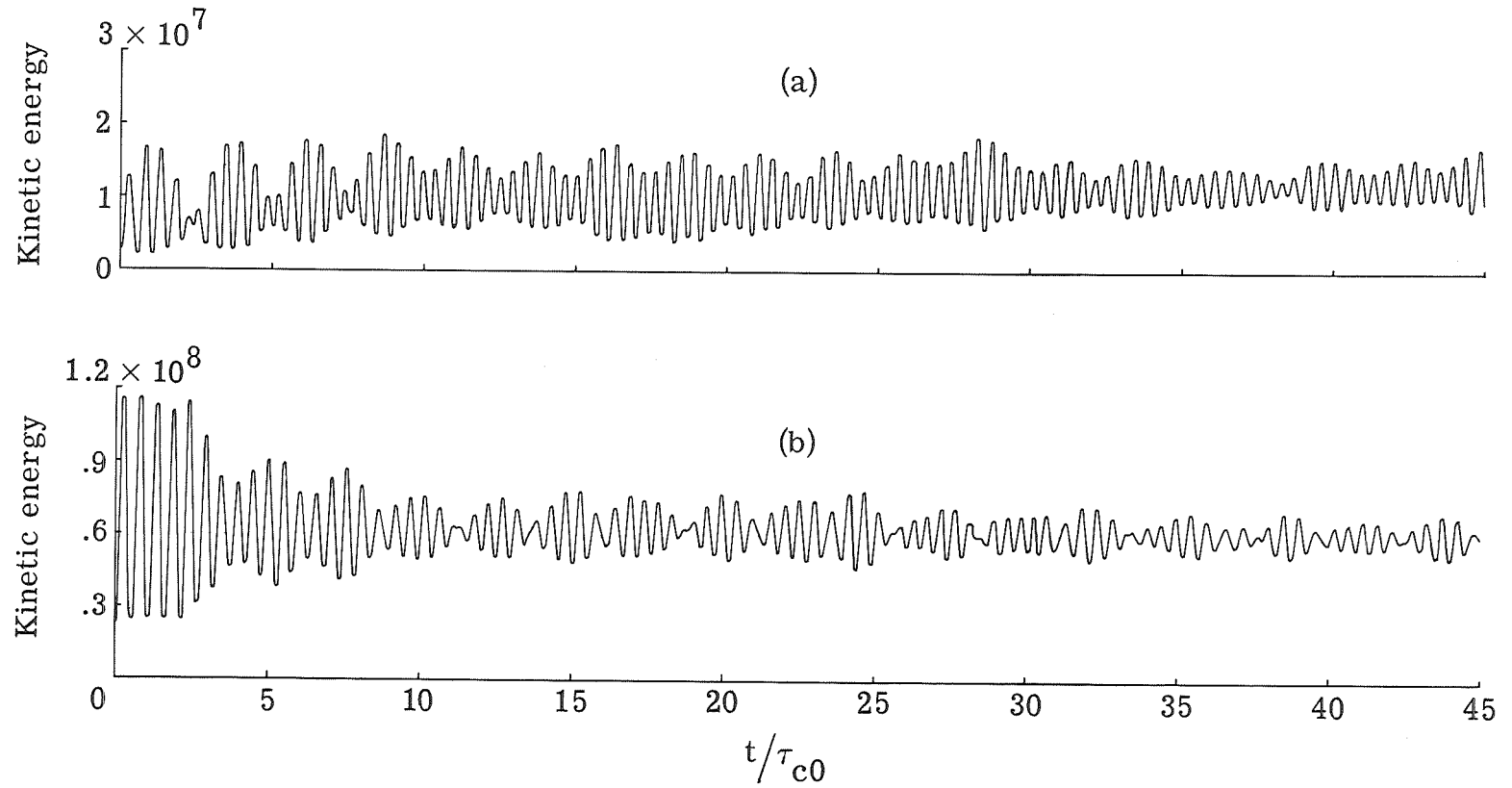
Figure 9.- Evolution of the kinetic energy for the system shown in figure 7. (a) Total kinetic energy corresponding to $\langle f_1 \rangle$ and (b) Total kinetic energy corresponding to $\langle f_2 \rangle$.
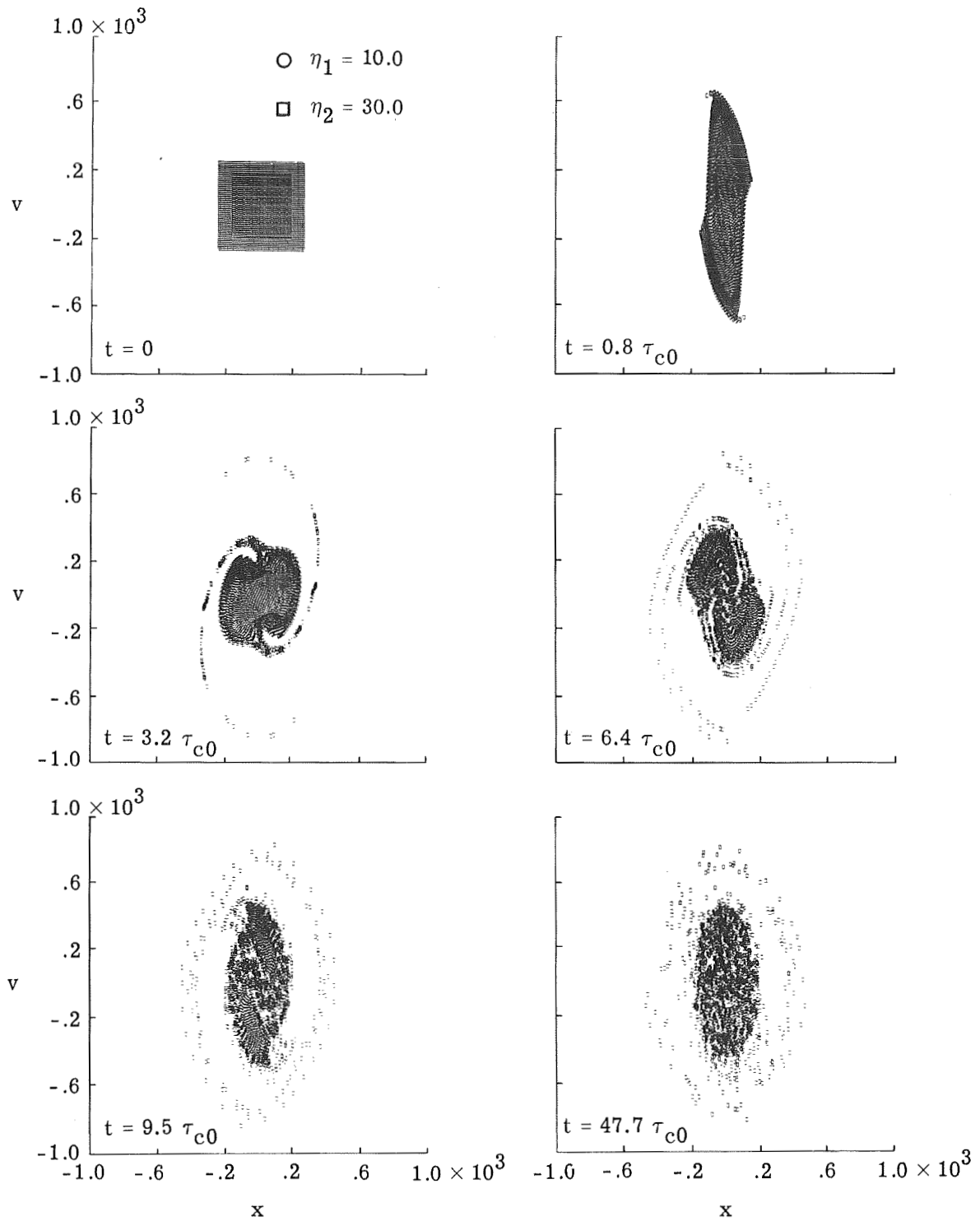
Figure 10.- Evolution of a two-phase-density system in phase space. The outer region has a phase density three times as large as that of the inner region.

Figure 11.- Comparison of the final distribution with the Lynden-Bell distribution for the system shown in figure 10. Inserts show the energy distribution.

Figure 12.- Evolution of the kinetic energy for the system shown in figure 10. (a) Kinetic energy corresponding to $\langle f_1 \rangle$ and (b) Kinetic energy corresponding to $\langle f_2 \rangle$.
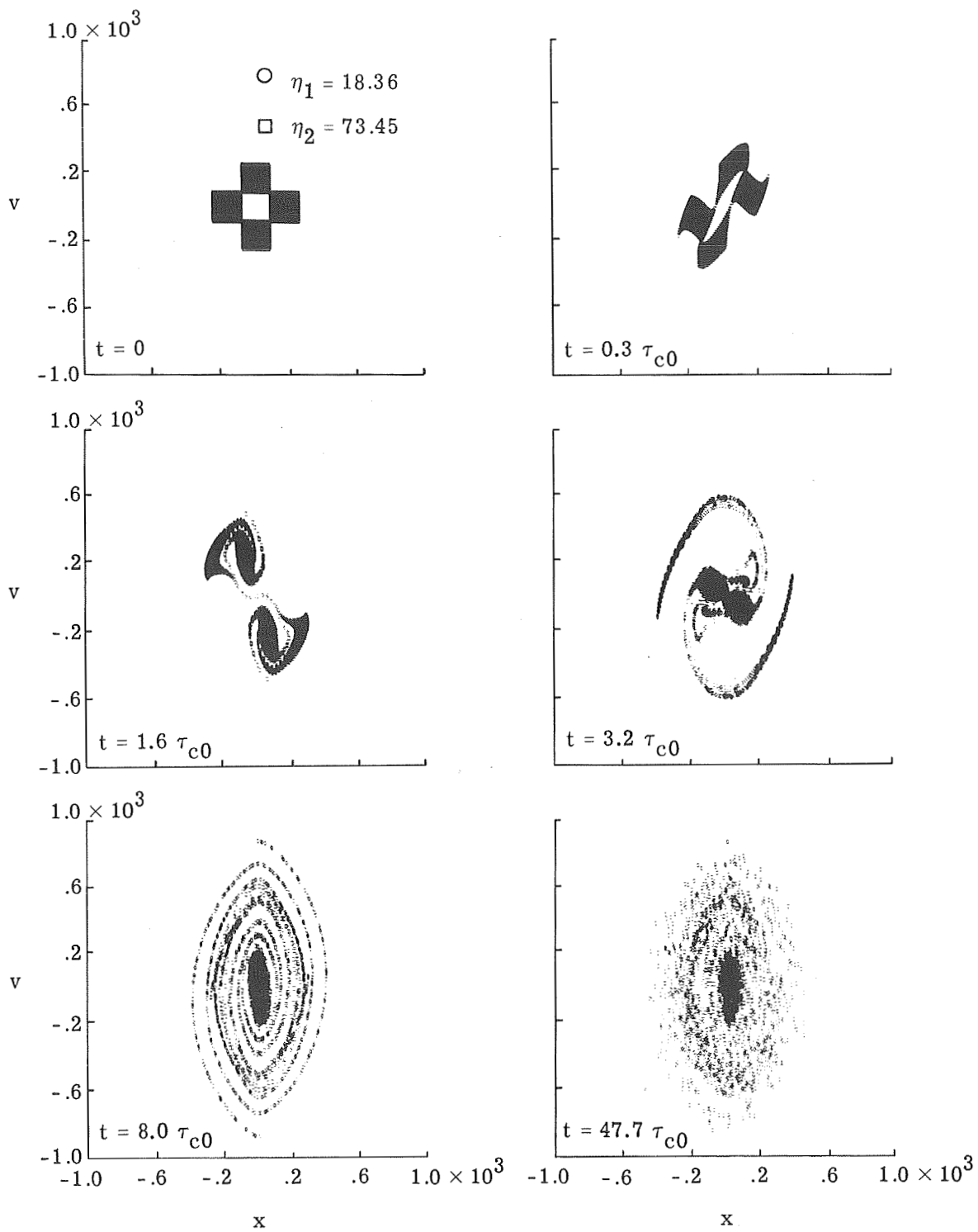
Figure 13.- Evolution of a two-phase-density system in phase space. The left and right rectangles have a phase density four times as large as the top and bottom rectangles.
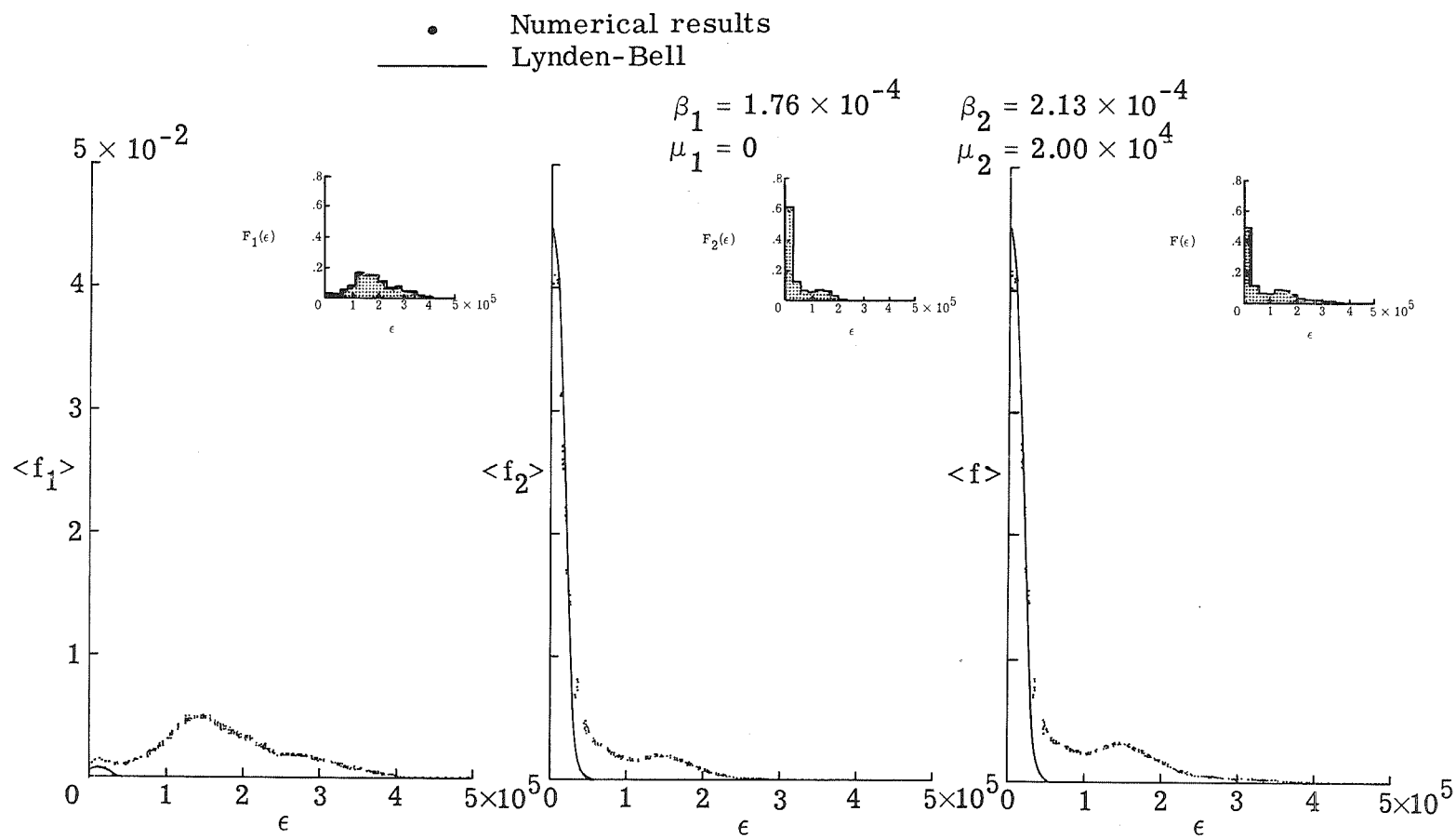
Figure 14.- Comparison of the final distribution with the Lynden-Bell distribution for the system shown in figure 13. Inserts show the energy distribution.

Kinetic energy

8×10^7

(a)

4

0

Kinetic energy

1.6×10^8

1.2

(b)

.8

.4

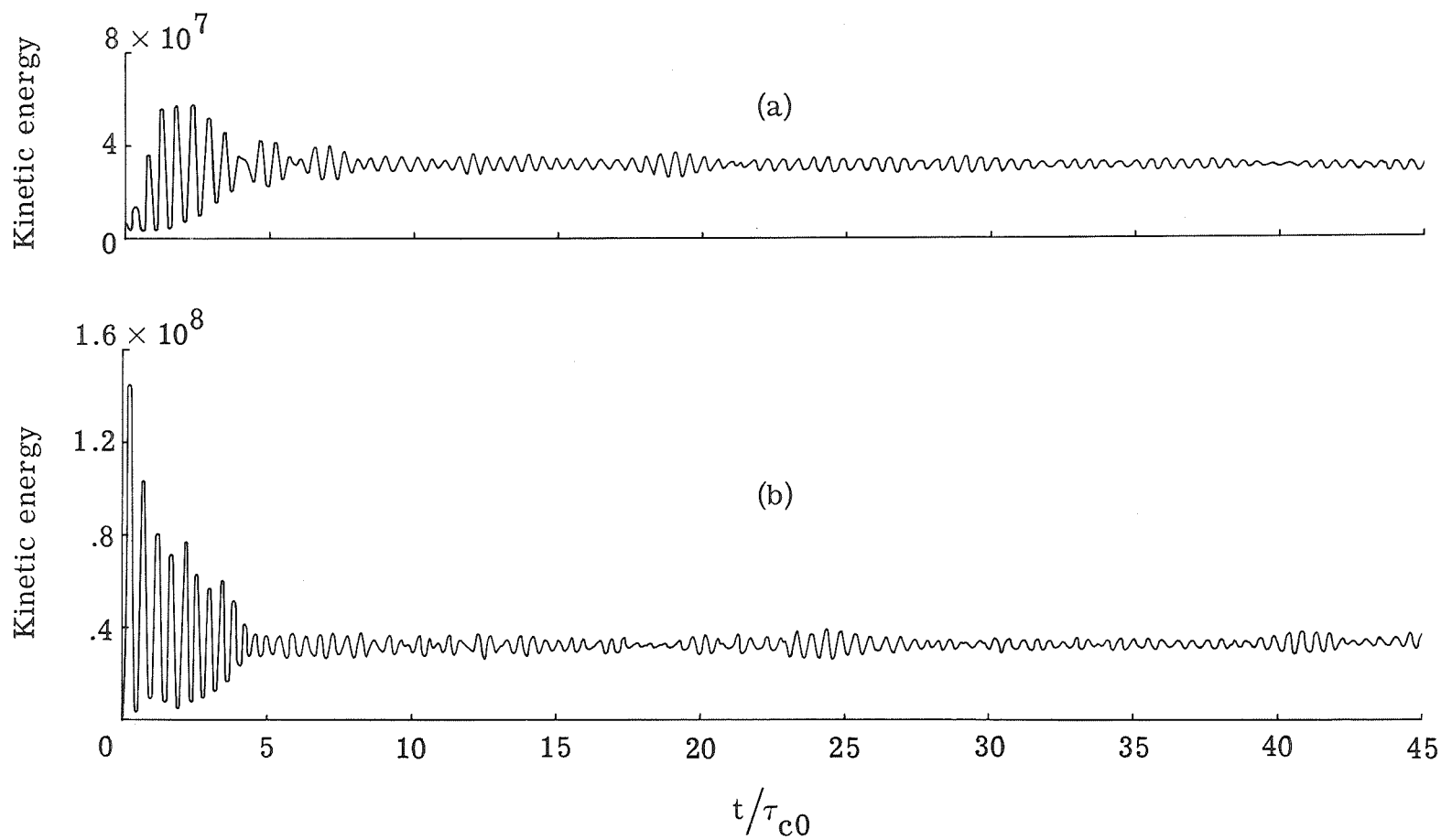0   5   10   15   20   25   30   35   40   45

t/τ_{c0}

Figure 15.- Evolution of the kinetic energy for the system shown in figure 13. (a) Kinetic energy corresponding to $\langle f_1 \rangle$ and (b) Kinetic energy corresponding to $\langle f_2 \rangle$.

FIRST CLASS MAIL

POSTMASTER: If Undeliverable (Section 158
Postal Manual) Do Not Return

> *"The aeronautical and space activities of the United States shall be
> conducted so as to contribute . . . to the expansion of human knowl-
> edge of phenomena in the atmosphere and space. The Administration
> shall provide for the widest practicable and appropriate dissemination
> of information concerning its activities and the results thereof."*
>
> — NATIONAL AERONAUTICS AND SPACE ACT OF 1958

NASA SCIENTIFIC AND TECHNICAL PUBLICATIONS

TECHNICAL REPORTS: Scientific and
technical information considered important,
complete, and a lasting contribution to existing
knowledge.

TECHNICAL NOTES: Information less broad
in scope but nevertheless of importance as a
contribution to existing knowledge.

TECHNICAL MEMORANDUMS:
Information receiving limited distribution
because of preliminary data, security classifica-
tion, or other reasons.

CONTRACTOR REPORTS: Scientific and
technical information generated under a NASA
contract or grant and considered an important
contribution to existing knowledge.

TECHNICAL TRANSLATIONS: Information
published in a foreign language considered
to merit NASA distribution in English.

SPECIAL PUBLICATIONS: Information
derived from or of value to NASA activities.
Publications include conference proceedings,
monographs, data compilations, handbooks,
sourcebooks, and special bibliographies.

TECHNOLOGY UTILIZATION
PUBLICATIONS: Information on technology
used by NASA that may be of particular
interest in commercial and other non-aerospace
applications. Publications include Tech Briefs,
Technology Utilization Reports and Notes,
and Technology Surveys.

Details on the availability of these publications may be obtained from:

SCIENTIFIC AND TECHNICAL INFORMATION DIVISION

NATIONAL AERONAUTICS AND SPACE ADMINISTRATION
Washington, D.C. 20546